Int. J. Electrochem. Sci., 12 **(2017)** 1034 – 1051, doi: 10.20964/2017.02.37

International Journal of
ELECTROCHEMICAL
SCIENCE
www.electrochemsci.org

Electrodeposition and Characterization of Co-W Alloy from Regenerated Tungsten Salt

Liwen Ma[*], *Xiaoli Xi, Zuoren Nie, Tingting Dong, Yuhui Mao*

College of Materials Science and Engineering, Beijing University of Technology, Beijing 100124, China
[*]E-mail: maliwen@bjut.edu.cn

Received: 31 August 2016 / *Accepted:* 9 December 2016 / *Published:* 30 December 2016

In this study, Co-W alloy was electrodeposited by regenerated sodium tungstate, cobalt sulfate and citric acid as complexing agent. Microhardness testing, XRF, XRD and SEM were used to characterize the properties of the alloy coatings. The optimal conditions for the electrodeposition were found as follows: sodium tungstate concentration 0.3mol/L, cobalt sulfate concentration 0.2mol/L, a current density of 500mA/dm^2, temperature of 60 ℃ and pH 5-7. Under the optimal conditions, the obtained alloy coating exhibits hardness of 550HV with smooth and compact morphology and deposition current efficiency of 65%. The prepared Co-W alloy using regenerated agent presents similar hardness compared to the alloy obtained from analytical grade materials by this complex electrodeposition process, indicating that the regenerated tungsten can be used to prepare qualified Co-W alloy coating.

Keywords: Electrodeposition; Co-W alloy; Complexation; Regenerated tungsten

1. INTRODUCTION

Decorative and functional chromium coating has been rapidly developed. However, the electrodeposition process is usually toxic and was restricted by some environmental protection rules [1]. Among some acceptable alternatives to electrolytic chromium coatings, the tungsten-iron group metals coatings are the most promising, as they offer a wide range of properties, such as high hardness, strength, and corrosion and wear resistances [2, 3]. So, they can be used in valves, dies, cutting tools, gas turbines, jet engines and injection molds [4, 5].

Tungsten belongs to the category of refractory metals with a very high melting point and very negative reduction potential. Pure tungsten can be electrodeposited from its florid melt, but cannot be electrodeposited from organic and/or aqueous solutions [6–9], unless it codeposits into an alloy with metals of the iron group. Aqueous solutions of tungstate together with an iron group metal were generally unstable; unless a suitable salt of a hydroxyl organic acid is also present [10]. Tungsten

alloys of iron group metals were electrodeposited from pyrophosphate [11], gluconate [12, 13] or citrate electrolytes [14-16] in crystalline, nanocrystalline and amorphous forms [17, 18]. The content, structure and morphology of the tungsten alloys depend on the electrodeposition conditions, such as the bath composition, pH, temperature and current density. However, with the recycling of tungsten arousing wide concerns in recent years, the usage of regenerated tungsten salt from spent catalysts, printed circuit board and waste carbide [19-21] gradually increases. But there is rare literature studied the electrodeposition process and the performance of Co-W alloy prepared by regenerated salt. Studies suggested that the W powder or WO_3 powder reduced by H_2 from regenerated salt show inferior performance, compared to products manufactured from analytical grade agent (primary material) [22], which may be attributed to the relatively low purity of the regenerated salt. During the electrodeposition process, the metal reduces in accordance with the deposition potential order on the cathode. It is theoretically possible to selectively precipitate the target metal, thus achieving purification for regenerated salt. To prepare Co-W alloy coating using regenerated tungsten salt, is expected to an approach for tungsten recycling with high performance. The procedure is also environmental friendly, resources saving and highly efficient for materials recycling.

This paper is designed to use the electrodeposition method by adding a complexing agent to prepare qualified Co-W alloy from regenerated salt, and research the effect of different factors during the preparation process. The different factors, such as current density, temperature and pH, were investigated and the hardness, structure, morphology and composition of the alloy were characterized.

2. EXPERIMENTAL PROCEDURE

2.1 Electrochemical testing

Table 1. Electrolytes composition for electrochemical testing (g/L)

Composition	Blank solution	Co Electrolyte	W Electrolyte	Co-W Electrolyte
$Na_2WO_4 \cdot 2H_2O$			99	99
$CoSO_4 \cdot 7H_2O$		56		56
$C_6H_8O_7 \cdot H_2O$	80	80	80	80
H_3BO_3	40	40	40	40
Sodium dodecyl sulfate	1	1	1	1

The cyclic voltammetry (CV) was conducted by an electrochemical workstation in a citric system at pH 5 at 25 ℃. The compositions of the electrolytes are presented in Table 1. Wherein citric acid works as a complexing agent to achieve codeposition of Co and W, boric acid and sodium dodecyl sulfate can improve the properties of the bath, and to some extent affect the deposition result. So, the cyclic voltammetry study is necessary to determine the electrodeposition behavior in this electrolyte system. A carbon electrode with efficient area of 3.5 mm^2 was the working electrode, a

platinum electrode with efficient area of 11 mm^2 was the counter electrode and a saturated calomel electrode was used as the reference electrode. The scan rate was set at 50mV/s.

Different conditions on the cyclic voltammetry of electrodeposition of Co-W alloy coating were studied. The effect of concentration of tungsten ions (0.1-0.6mol/L) was studied at Co^{2+}=0.2mol/L, pH=5, 25℃, scan rate of 50mV/s; the effect of temperature (30-60℃) was studied at WO_3^{2-}=0.3mol/L, Co^{2+}=0.2mol/L, pH=5, scan rate of 50mV/s; the effect of pH (3-9) was studied at WO_3^{2-}=0.3mol/L, Co^{2+}=0.2mol/L, 25℃, scan rate of 50mV/s.

2.2 Electrodeposition

The Co-W alloy coating was prepared on a stainless steel substrate with two graphite plates as anodes by galvanostatic electrodeposition on a DC power supply (E3610A, Agilent Technologies, Germany). The stainless steel sheet substrate was polished by 400, 600 and 800 mesh sandpaper, successively. The substrate was then washed with alkali solution, to remove any adhering grease, dust or other contaminants and placed into anhydrous for ultrasonic cleaning for 5-10 minutes. Finally, it was rinsed with 5% hydrochloric acid solution for 30-60s, to remove the oxide film produced during the early pretreatment. The electrolysis system was assembled as follows. A soft plug was fixed on a 150mL beaker. A metallic hook was set in the middle of the plug with the perforated stainless steel cathode with immersed area of 800mm^2 hanging on the hook. On both sides of the cathode, there fixed two perforated graphite plates as anodes on the plug. The wire was used to connect the anodes and cathode. Two graphite anodes can provide a uniform distribution of the electric field towards the cathode.

The electrolyte composition is presented in Table 2. Wherein the sodium tungstate was produced by the reaction between sodium hydroxide and tungsten oxide, which was calcined by ammonium paratungstate (APT), recovered from spent catalysts. Thus, the obtained coatings were denoted as "regenerated coatings". Different values of pH (3-9), temperature (40-80℃) and current density (170-1000 mA/dm^2) were investigated during the electrodeposition process for 3 h. In the process of electrodeposition, the other experimental conditions were pH 7, 60 ℃ and 500 mA/dm^2 when a certain factor changed.

Table 2. Electrolyte composition used for electrodeposition (g/L)

Composition	Concentration
Na_2WO_4	99
$CoSO_4 \cdot 7H_2O$	56
$C_6H_8O_7 \cdot H_2O$	80
H_3BO_3	40
Sodium dodecyl sulfate	1

The Co-W coatings (primary coatings) were also prepared under the above experimental conditions by analytical grade agent.

2.3 Characterization Techniques

An electrochemical workstation (PARSTAT4000, Princeton Applied Research, U.S.) was used to perform electrochemical testing. An X-ray fluorescence spectrometer (XRF, XRF-1800, Shimadzu, Japan) was used to analyze the composition of Co-W alloy. The surface morphology of the alloy was characterized by a field emission scanning electron microscope (SEM, Hitachi, SU8020, Japan). A micro hardness tester (HXD-100TMC/LCD, Shanghai Taiming Optical instrument Co., Ltd. China) was used to measure the hardness of coatings. The structures of the coatings were investigated by an X-ray diffraction spectrometer (XRD, 7000 S/L, Rigaku, Japan) with a Cu anticathode (Cu $K\alpha$ radiation λ= 1.54056 Å) at room temperature. The measurements were recorded under Bragg-Brentano geometry at 2θ with step of 10°/min in the range of 10–90°.

3. RESULTS AND DISCUSSION

3.1 Electrochemical testing

The cyclic voltammetry curves for the different electrolytes in our study are presented in Fig. 1. As can be observed from Fig. 1 (a), in the solution containing no cobalt and tungstate ions, the cyclic voltammetry curve only exhibits the hydrogen evolution reaction without any other redox peaks. However, in the curves of the cobalt-containing solution, a reduction peak appears at -0.65V, as observed in Fig. 1 (b), corresponds to the cobalt deposited on the cathode. Fig. 1 (c) shows no metal redox peaks on the cyclic voltammetry curve because the electrolyte only contains tungsten, which cannot be electrodeposited on the cathode in an aqueous solution, due to its negative standard electrode potential. The electrochemical reduction of WO_4^{2-} ion occurs as follows.

$$WO_4^{2-} + 8H^+ + 6e^- \rightarrow W + 4H_2O \quad (1)$$

The standard potential is given by equation (2). At pH 9, [WO_4^{2-}] = 0.1 M and E = −0.679 V vs SHE. The reduction of [WO_4^{2-}] to W depends mainly on the potential.

$$E = 0.049 - 0.0788\ pH + 0.0098\ log\ [WO_4^{2-}] \quad [23]$$

(2)

It is observed from Fig. 1 (d) that in the electrolyte containing Co and W, a reduction peak appears at -0.8 V. As tungsten can be induced to the coelectrodeposit by the iron group metals [10], the peak at -0.8v likely corresponds to the electrodeposition of Co-W alloy on the cathode. Complexes of tungstates with citrates are known with the general formula $[(WO_4)(Cit)(H_x)]^{x-5}$, where (Cit) stands for the triply deprotonated anion of citric acid concentration and x is the number of protons [24, 25]. According to the references [26-29], regarding Ni-W alloy electrodeposition, there are many different coordination forms of Ni and W within citrate electrolyte. They can be transformed into each other, such as:

$$\left[(Ni)(Cit)\right]^- + \left[(WO_4)(Cit)(H)\right]^{4-} \rightarrow \left[(Ni)(WO_4)(Cit)(H)\right]^{2-} + Cit^{3-} \quad (3)$$

$$\text{or } \left[(Ni)(WO_4)(Cit)(H)\right]^{2-} + \left[(WO_4)(Cit)(H)\right]^{4-} \rightarrow \left[(Ni)(WO_4)_2(H)_2(Cit)\right]^{3-} + Cit^{3-} \quad (4)$$

The tungstate-citrate complex forms a complex with nickel citrate in the bulk of the solution or on the surface and the ternary complex of the type $[(Ni)(WO_4)(Cit)(H)]^{2-}$ is the precursor for the deposition of the Ni-W alloy.

The relationships between solution chemistry and electrodeposition of Co-W alloys coatings, produced from a gluconate bath, were studied by D.P. Weston [22]. The presence of various species was proved to exist in the complex bath, such as the non-complexed Co^{2+}, poly and meta-tungstates, hetero-polytungstate species containing cobalt, tungstate-gluconate, cobalt-gluconate, cobalt-tungstate gluconate, and cobalt-paratungstate-gluconate species. So, similarly in our citrate electrolyte, it was speculated to exhibit a variety of reducible non-complexed or complexed cobalt-tungstate-citrate species. The decomposing of these species depends on the deposition potential and its concentration. The presence of the mixed cobalt-paratungstate-gluconate is believed to be important for gaining high W alloy deposits at high deposition efficiencies [22]. To refer to the above results, it is speculated that the cathode reaction of the present study can be simplified into the two equations (5) and (6), according to the literature [30]. From these, equation (5) is the main reaction and equation (6) is the side reaction.

$$[Co(HWO_4)(Cit)]^{2-} + 3H_2O + 8e^- \rightarrow CoW + 7(OH)^- + Cit^{3-} \quad (5)$$

$$2H^+ + 2e^- \rightarrow H_2 \uparrow \quad (6)$$

Usually, the reduction potential of a cobalt complex is more negative than Co^{2+}. $[(Co)(HWO_4)(Cit)]^{2-}$ can be considered as tungstate being a ligand of Co, by replacing some amount of citrate, the reduction potential of the Co-W alloy is also expected to be more negative than Co^{2+}.

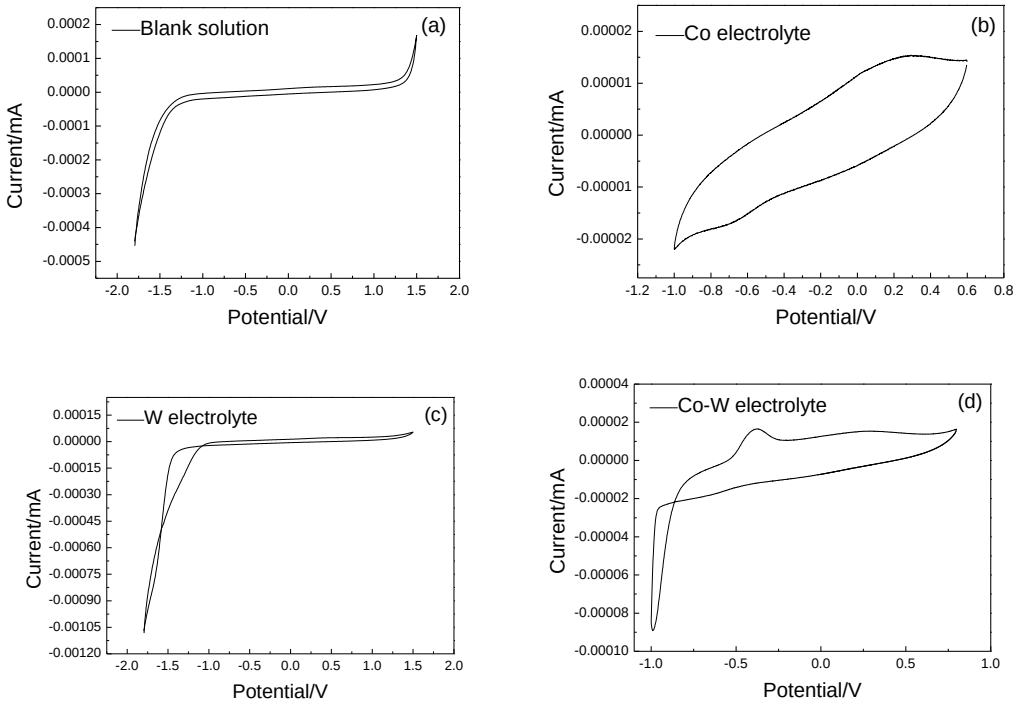

Figure 1. Cyclic voltammetry curves for different electrolytic systems: (a) Blank solution; (b) Co electrolyte (congtaining $CoSO_4 \cdot 7H_2O$ 56 g/L); (c) W electrolyte (congtaining $Na_2WO_4 \cdot 2H_2O$ 99 g/L); (d) Co-W electrolyte (congtaining $CoSO_4 \cdot 7H_2O$ 56 g/L, $Na_2WO_4 \cdot 2H_2O$ 99 g/L) experimental conditions: pH 5, 25 ℃, scan rate 50mV/s.

Fig.2 shows the effect of tungsten concentration, temperature and pH on the electrodeposition behavior of Co-W alloy. As can be seen from Fig. 2 (a), the reduction peak of Co-W alloy firstly shifts positively and then negatively with the WO_4^{2-} concentration increases, indicating that the coelectrodeposition of W and Co can be promoted at a suitable amount of tungsten concentration of about 0.3mol/L. As the temperature increases (seen from Fig. 2 (b)), the reduction peak of Co-W alloy constantly moves in the positive direction, indicating that the rising temperature is in favor of the electrodeposition of Co-W alloy. The cathodic reduction potential in Fig. 2 (c) shifts negatively with the increase of pH. The reductions are primarily hydrogen evolution reaction in addition to the codeposition of alloy. So the hydrogen evolution reaction occurs more difficultly when pH increases, which is favor to the occurrence of the electrodeposition reaction.

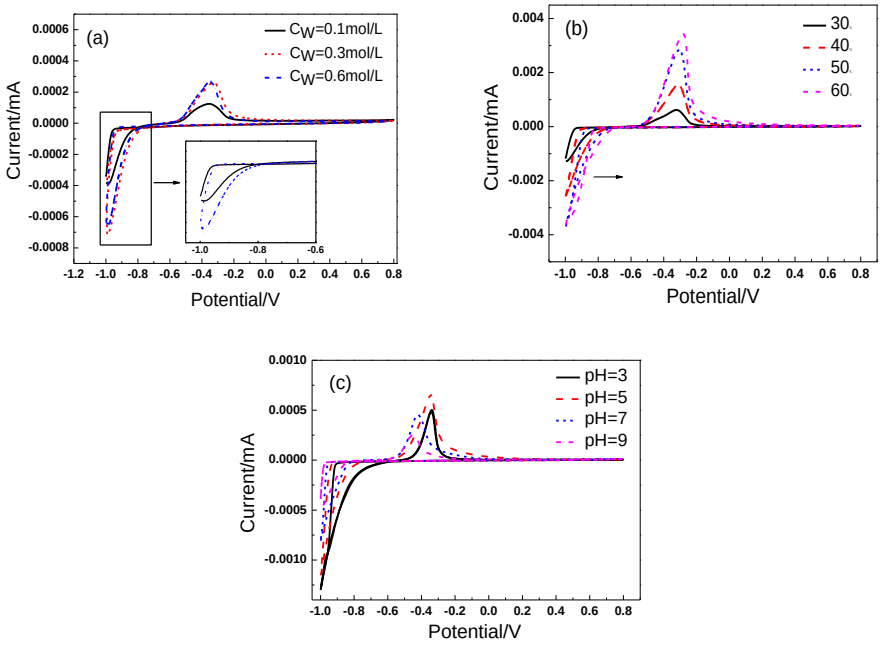

Figure 2. Effect of different factors on cyclic voltammetry curve: (a) W concentration of 0.1-0.6 mol/L (Co^{2+} 0.2mol/L, pH 5, 25℃, scan rate 50mV/s); (b) temperature of 30-60℃(WO_3^{2-} 0.3mol/L, Co^{2+} 0.2mol/L, pH 5, scan rate 50mV/s); (c) pH of 3-9 (WO_3^{2-} 0.3mol/L, Co^{2+} 0.2mol/L, 25℃, scan rate 50mV/s).

3.2 Effect of current density on electrodeposition

Current density will affect the deposition rate, current efficiency, composition of alloy coating and hardness. The Co-W alloy was electrodeposited by regenerated Na_2WO_4 at pH 7 at a temperature of 60 ℃ for 3h, with current densities varying between 170-1000 mA/dm^2. Fig. 3-5 show the relationship between current density and the above factors.

Since the Co and W have different deposition rate and quality during electrodeposition, we use the deposited mass of the alloy per unit area of cathode on a certain time to characterize the overall electrodeposition rate of the alloy. With the increase of current density, the Co-W alloy deposition rate is initially gradually increased and then decreased, reaching its maximum value of 3.487 g/ (m^2·h) at a current density of 500 mA/dm^2. The current efficiency shows similar changing trend with the

deposition rate, however the rate of changing is slightly different. According to Faraday's law, the greater the current, the more the charge that passes through the cathode, and so the more the amount of metal deposited on the substrate, thus, the deposition rate is increased. When the current density becomes too high >500 mA/dm^2, the rate of the whole electrode process is primarily controlled by the metal ion diffusion towards the surface of the cathode. This results into a significant lack in metal ions, enhances hydrogen evolution and finally leads to the difficulty of metal deposition and to a decrease of the deposition rate. Current efficiency is basically positively correlated to the trend of the deposition rate.

The current efficiency of the alloy was calculated as:

$$Current\ efficiency(\%) = \frac{M \times 100}{e_{alloy} \times Q} \tag{7}$$

Where M is the mass of the alloy deposit, e_{alloy} is the electrochemical equivalent of the alloy and Q is the quantity of electricity passed through the electrode (A/s). The electrochemical equivalent of the alloy was calculated as:

$$e_{alloy} = \frac{e_{Ni} \times e_W}{e_{Ni} \times f_W + e_W \times f_{Ni}} \tag{8}$$

Where e_{Ni} and e_W are the electrochemical equivalents of the constituent metals, and f_{Ni} and f_W are their fractions in the coatings [31].

The W content (wt.%) of the coating is firstly increased and then decreased, as the current density is increasing. The W content reaches the highest value of 44.2 wt.% at a current density of 500mA/dm^2. This means that relatively high current density favors the reduction of tungsten ions and increases the W content. As the reduction of alloy is correlated to the difference in static potential of the constituent metals [32], there is a higher difference between the static potentials of Co and W at lower current density values. Thus, relatively high current density favors the codeposition of Co and W. However, too high current density for the cathode (> 500 mA/dm^2) will enhance hydrogen evolution, consequently increasing the pH values. This may further result into the destruction of the active complexed cobalt-tungstate-citrate species, the inhibition of the discharge of the tungsten and the reduction of the W content of the coating. The trend of Co is reverse from that of W.

The hardness of the coating was significantly enhanced by increasing current density (< 500 mA/dm^2). The electrodeposited Co-W alloy is a substitution solid solution, having a face-centered cubic structure, with Co being the solvent and W the solute. The tungsten occupies the cobalt positions in the matrix and lattice distortion is generated. Hence, the resistance increases when the dislocations of the deposits slip, which increases the hardness of the alloy. W content is not the only factor affecting the microhardness of the coating. The increase of the current density is in favor of the cathodic depolarization, which favors the formation of nuclei in the Co-W alloy, further resulting into a reduced average grain size, thereby increasing the overall hardness. Tungsten can enhance the hardness of Co-W alloys due to various strengthening effects, such as solid solution strengthening, grain refining strengthening, or second phase strengthening [12]. When the current density >500 mA/dm^2, the W content and the hardness were decreased. The optimal current density is approximately 500mA/dm^2.

The above results were similar to those of the literatures [30, 33]: current efficiency and W content firstly increased and then decreased with increasing current density. Co-W alloy shows similar performance with Ni-W alloy. Literature [30] reported that Ni-W alloys were electrodeposited on mild steel from ammonical citrate complexing bath. Increasing of peak current density from 1 to 3 A/dm^2 has increased the current efficiency to 50.8% and content of W to 32.25% in the alloy. However, beyond 3 A/dm^2, there was a decrease of current efficiency and W content. Literature [33] revealed that when the current density increased from 0.5 to 5 A/dm^2, the variation of current efficiency and W content for Co-W alloy were related to the pH of the bath. The current efficiency reached highest about 82% at pH 6 at current density of 0.5 A/dm^2 and lowest about 10% at pH 8 at current density of 4 A/dm^2. The significant variation for the findings in other literatures and this paper was attributed to the differences in the reaction kinetics at different pH in terms of the adsorption steps taking place at the electrode. The electrode reaction involves at least three conjugated electrochemical processes, namely Co(II) and W(VI) reduction, and hydrogen evolution. These net reactions involve a multi-electron transfer with the adsorption of intermediates (eg. active metal-complexed species). These factors affected each other, so that the current efficiency and tungsten content fluctuated with respect to current density.

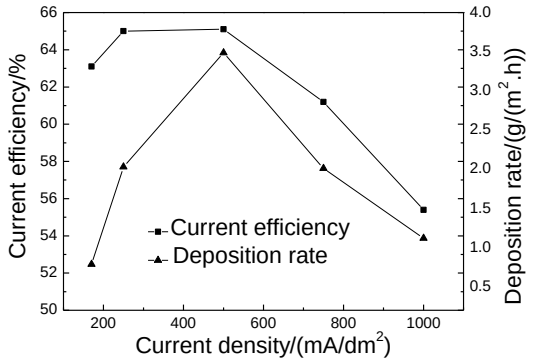

Figure 3. Effect of current density (170-1000 mA/dm^2) on the deposition rate and current efficiency for electrodepostion of Co-W coatings; experimental conditions: (g/L)Na_2WO_4 99, $CoSO_4 \cdot 7H_2O$ 56, $C_6H_8O_7 \cdot H_2O$ 80, H_3BO_3 40, Sodium dodecyl sulfate 1, pH 7, 60 ℃.

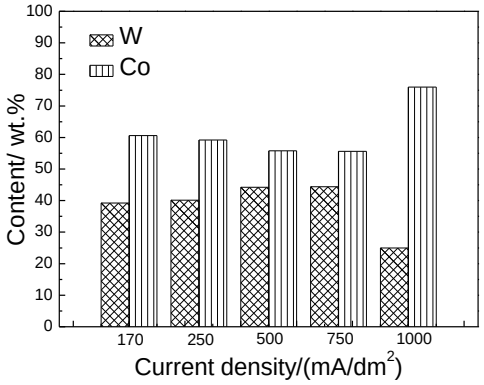

Figure 4. Effect of current density (170-1000 mA/dm^2) on the contents of W or Co of coatings; experimental conditions: (g/L)Na_2WO_4 99, $CoSO_4 \cdot 7H_2O$ 56, $C_6H_8O_7 \cdot H_2O$ 80, H_3BO_3 40, Sodium dodecyl sulfate 1, pH 7, 60 ℃.

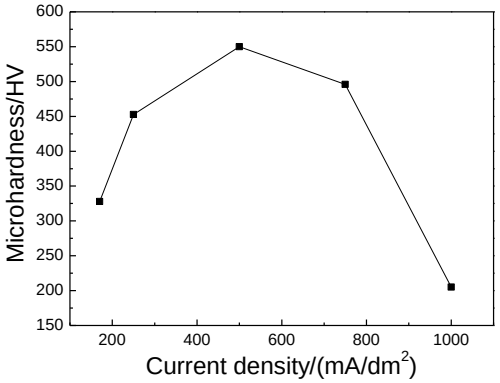

Figure 5. Effect of current density (170-1000 mA/dm^2) on hardness of Co-W coatings; experimental conditions: (g/L)Na_2WO_4 99, $CoSO_4 \cdot 7H_2O$ 56, $C_6H_8O_7 \cdot H_2O$ 80, H_3BO_3 40, Sodium dodecyl sulfate 1, pH 7, 60 ℃.

3.3 Effect of temperature on electrodeposition

Temperature will affect the deposition rate, current efficiency, composition of alloy coating and hardness. The Co-W alloy was electrodeposited for 3h by regenerated Na_2WO_4 at pH 7 at the temperature range between 40-80 ℃, at current density of 500 mA/dm^2. Fig. 6-8 show the relationship between temperature and the above factors.

As the temperature increases from 40 ℃ to 80 ℃, the electrodeposition rate first increases to its maximum value at 60 ℃, and then decreased. This change of the current efficiency is similar to that of the deposition rate, with its highest value recorded for 65 % at 60 ℃. The temperature increase leads to the increase of the diffusion rate of the reducible metal-containing complexes and their migration, which reduces the cathodic polarization. This means that the concentration of the reducible complexed cobalt-tungstate-citrate species in the cathode diffusion layer should be increased, the electrochemical activity of the complexes is enhanced and the codeposition of W and Co should be promoted. Thus, the deposition rate and current efficiency increase. This result was similar to that reported in literature [30]. The bath temperatures were increased to enhance the mass transport. Increase of temperature could increase the current efficiency. However if the temperature becomes too high above 60 ℃, the decomposition of citric acid, active metal-complexed species and other additives might occur, which is not favor to alloy codeposition, and the deposition rate and the current efficiency will therefore decrease.

The W content (wt.%) of the coating initially increases by increasing the temperature until 60 ℃, reaches a maximum of 44.2 wt.% and then decreases. This behavior indicates that the increasing temperatures are probably beneficial for the generation, migration and discharge of the complexed cobalt-tungstate-citrate species, which reduces the cathodic polarization and promote tungsten precipitation. Consequently, the W content in the alloy increases. When the temperature is too high > 60 ℃, the form of complexed species is speculatedly changed and the concentration of tungsten-containing complexes may be reduced. In addition, the additive is also easier to break down and the electrolyte is unstable, which is not favor to the codeposition of tungsten. The increasing temperature

was in general to promote the electrodeposition process. But as the electrodeposition was affected by many factors, changes in temperature would affect the composition of the alloy through the change of the discharge species, the mechanism and rate of the net electrochemical reactions. The W content might fluctuate in the alloy [29].

The hardness of the alloy is increased to 550HV when temperature ≤ 60 ℃, and then decline. The hardness trends are consistent with the W content, indicating that an increase of W content will improve the alloy hardness. 60 ℃ is considered as a suitable temperature for electrodeposition of Co-W alloy.

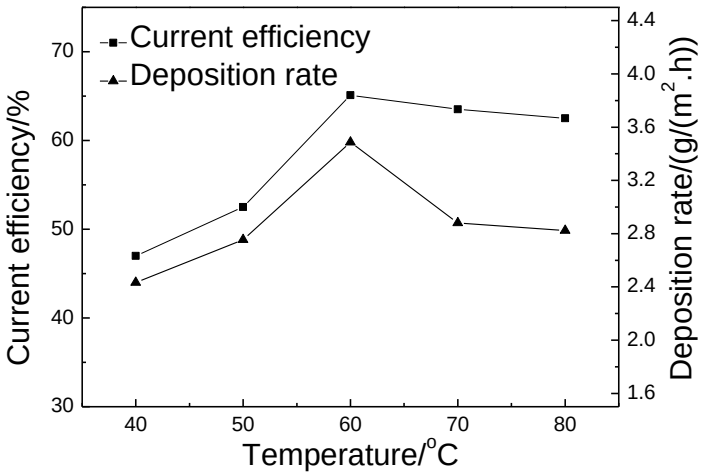

Figure 6. Effect of temperature (40-80 ℃) on deposition rate and current efficiency for electrodepostion of Co-W coatings; experimental conditions: (g/L)Na_2WO_4 99, $CoSO_4 \cdot 7H_2O$ 56, $C_6H_8O_7 \cdot H_2O$ 80, H_3BO_3 40, Sodium dodecyl sulfate 1, pH 7, 500 mA/dm^2.

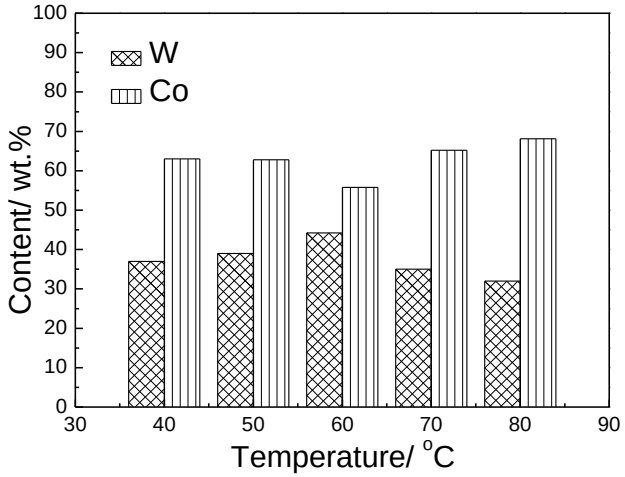

Figure 7. Effect of temperature (40-80 ℃) on the contents of W or Co of coatings; experimental conditions: (g/L)Na_2WO_4 99, $CoSO_4 \cdot 7H_2O$ 56, $C_6H_8O_7 \cdot H_2O$ 80, H_3BO_3 40, Sodium dodecyl sulfate 1, pH 7, 500 mA/dm^2.

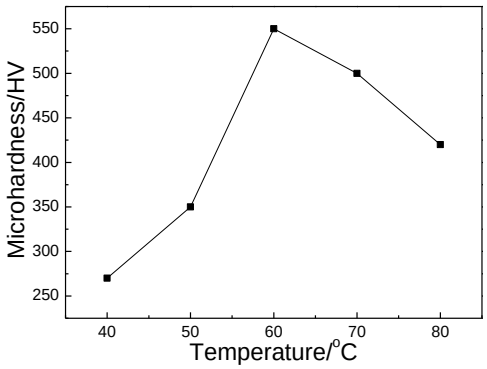

Figure 8. Effect of temperature (40-80 ℃) on hardness of Co-W coatings; experimental conditions: (g/L)Na_2WO_4 99, $CoSO_4 \cdot 7H_2O$ 56, $C_6H_8O_7 \cdot H_2O$ 80, H_3BO_3 40, Sodium dodecyl sulfate 1, pH 7, 500 mA/dm^2.

3.4 Effect of pH on electrodeposition

The pH will affect the deposition rate, current efficiency, composition of alloy coating and hardness. The Co-W alloy was electrodeposited by regenerated Na_2WO_4 for 3h at the temperature of 60 ℃, at current density of 500 mA/dm^2, at different pH. Fig. 9-11 show the relationship between pH and the above factors.

As pH was increased from 3 to 9, the deposition rate was initially increased and then decreased, reaching a maximum value at pH 7. pH has a significant impact on the complex form of cobalt-tungstate-citrate species in the electrolysis system. Different coordination forms of cobalt and tungstate have different degrees of difficulty for electrodeposition. At lower pH values, the rate of migration and reduction of hydrogen ions in the electrolyte is substantially faster than that of the metal ions, the hydrogen evolution reaction is severe, and thus the deposition rate and current efficiency decrease. As pH values increase, the hydrogen evolution reaction is suppressed, the deposition rate and current efficiency are increased. The formation of complexed cobalt-tungstate-citrate species changes with pH. It may be relatively easy to form cobalt hydroxide or other non-tungsten complexes at pH 9 and the tungsten-containing complex dissociates. Hence, the deposition of the heavy metal W decreases, which reduces the quality of the coating and decreases the deposition rate.

The W content (wt.%) of the coating initially shows an increasing trend and then decreases with the increase of pH. At approximately pH 7, the W content reaches a maximum value of. 44.2 wt.%. When pH > 7 the W content decreases, the Co content has the reverse trend of W. This might be attributed to the fact that the pH has a great influence on the form of complexed cobalt-tungstate-citrate species. It is beneficial for tungsten deposition at pH < 7, and the W content of coating increases. When pH > 7, the excessive hydroxide ions react with cobalt to form cobalt hydroxide, decreasing the fraction of cobalt-tungstate-citrate species, which may be the reason for the decreased W content in alloy. The change of W and Co content of the coating is consistent with the variation of the deposition rate and current efficiency. Literature [34] revealed that the reaction kinetics was different at different pH in terms of the adsorption steps taking place at the electrode, and the

adsorption steps were affected by tungstate-containing complexes. In general, the stronger adsorption of the tungstate-containing complexes facilitated the tungstate reduction reaction at increased pH, and thus the content of W in Co-W alloys increased. However, the pH value also affected the ratio of cobalt-containing complexes and other species, and the deposited alloy of different compositions could affect the overvoltage for hydrogen evolution. The higher W content in the alloy usually caused a lower overvoltage for hydrogen evolution, and reduced the current efficiency [35]. Therefore, the W content and current efficiency may decrease as the pH increased when pH beyond a certain value [29, 30, 33].

The trends of hardness of the coating are basically consistent with that of W content. Low pH causes the significant hydrogen evolution and results in low W content and low hardness. During the electrodeposition process, it was observed a large number of bubbles on the cathode and the coating with visually pinholes at low pH. However, if the pH is too high (pH>7), the hardness was also decreased, which may be attributed to the decrease of W content and some mixed hydroxide precipitate in the coating. The maximum microhardness of 550 HV can be reached at pH 7. It is worth mentioning that the hardness is not only related to the W content, but also to morphology or grain size.

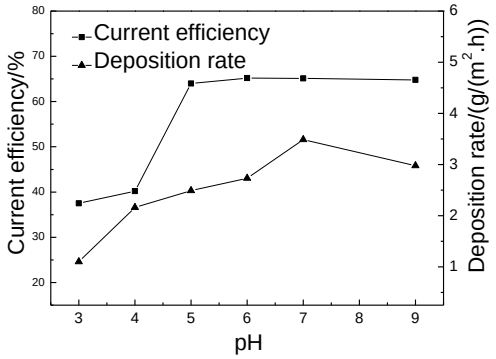

Figure 9. Effect of pH (3-9) on deposition rate and current efficiency for electrodepostion of Co-W coatings; experimental conditions: (g/L)Na_2WO_4 99, $CoSO_4 \cdot 7H_2O$ 56, $C_6H_8O_7 \cdot H_2O$ 80, H_3BO_3 40, Sodium dodecyl sulfate 1, 60 ℃, 500 mA/dm^2.

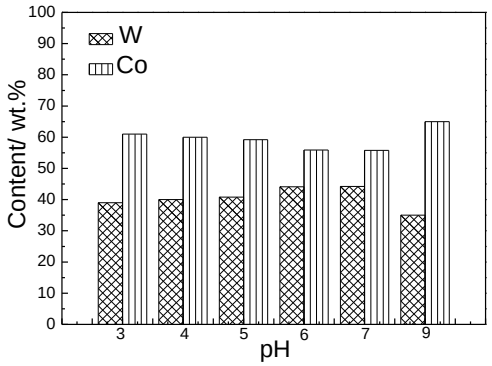

Figure 10. Effect of pH (3-9) on the contents of W or Co of coatings; experimental conditions: (g/L)Na_2WO_4 99, $CoSO_4 \cdot 7H_2O$ 56, $C_6H_8O_7 \cdot H_2O$ 80, H_3BO_3 40, Sodium dodecyl sulfate 1, 60 ℃, 500 mA/dm^2.

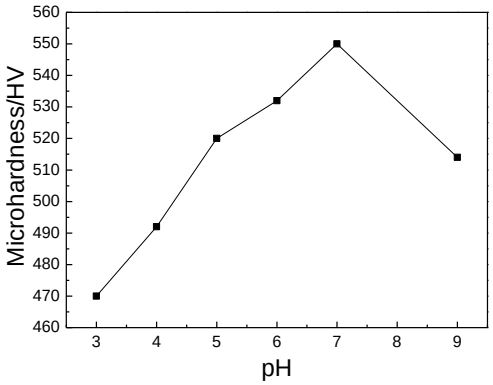

Figure 11. Effect of pH (3-9) on hardness of Co-W coatings; experimental conditions: (g/L)Na_2WO_4 99, $CoSO_4 \cdot 7H_2O$ 56, $C_6H_8O_7 \cdot H_2O$ 80, H_3BO_3 40, Sodium dodecyl sulfate 1, 60 ℃, 500 mA/dm^2.

3.5 Structure and morphology of the Co-W alloy coating

X-ray diffraction was used to analyze the structure of the Co-W alloy coatings obtained at various pH values. The results are presented in Fig. 12. When the pH is 3, 4, 5 or 9, their three strongest peaks position are: $2\theta_1$ = 44.580 °, $2\theta_2$ = 50.797 °, $2\theta_3$ = 74.751 °; $2\theta_1$ = 44.593 °, $2\theta_2$ = 50.850 °, $2\theta_3$ = 74.763 °; $2\theta_1$ = 44.460 °, $2\theta_2$ = 51.069 °, $2\theta_3$ = 74.643 °; $2\theta_1$ = 44.541 °, $2\theta_2$ = 50.820 °, $2\theta_3$ = 74.744 °, respectively. The three strongest peaks of pure Co were located at $2\theta_1$ = 44.62 °, $2\theta_2$ = 51.94 °, $2\theta_3$ = 76.14 °, while for pure W at $2\theta_1$ = 40.26 °, $2\theta_2$ = 58.36 °, $2\theta_3$ = 70.14 °. It is clear that Co-W alloy has crystalline peaks adjacent to the pure Co, indicating that W was embedded into the Co lattice by forming a substitutional solid solution with Co as solvent and W as the solute. This structure will produce local lattice distortions, resulting in the preferred hexagonal close-packed (hcp) lattice orientation or peak position shift. The three strongest peaks of the samples correspond to the crystal planes of (002), (101) and (110). Preferentially orientation in different planes will also affect the hardness of the coating [36]. A peak of 2θ at approximately 50° for the samples with pH = 3, 4, 5 or 9 is an unknown peak which was also reported in the literature [37]. The Bragg formula can describe the relationship between the change in lattice spacing d and the peak position of θ, as follows:

$$2d\sin\theta = n\lambda \tag{9}$$

From equation (9), it is known that if d increases, θ decreases. According to the peak position and the half width of the peak, the grain size can be calculated by the Scherrer equation (Eq. (10)).

$$L = \frac{k\lambda}{\beta\cos\theta} \tag{10}$$

Where, L is the average grain size; k is a constant that generally takes the value of 0.89; λ is the X-ray wavelength of 0.15406 nm; β is the half width of the peak and θ is the half value of the diffraction angle.

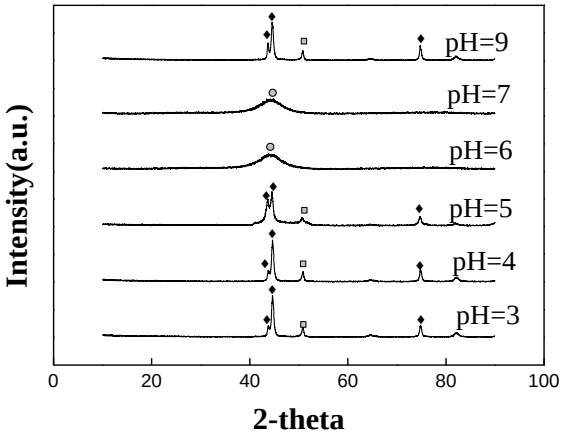

Figure 12. XRD patterns of the coatings obtained at various pH values ((g/L)Na_2WO_4 99, $CoSO_4 \cdot 7H_2O$ 56, $C_6H_8O_7 \cdot H_2O$ 80, H_3BO_3 40, Sodium dodecyl sulfate 1; pH=3-9; 60 ℃; 500 mA/dm^2).

Table 3 lists the peak position and the half width of the peak (FWHM) of the calculated grain size of the four crystal samples. As can be observed from Table 3, the average grain size of the sample at pH 5 is about 17 nm, the minimum of the four, which is consistent with the hardness results. The Co-W coatings electrodeposited on copper substrate were reported as single phase solid solution with an average grain size of about 18 nm [38]. It is known from the Hall-Petch formula (Eq. (11)) that the strength of the coating is inversely proportional to the square root of the apparent grain diameter; the smaller the grain the higher the intensity achieved and the higher the hardness of the coating. In the present study, the hardness is increased with the decrease of average grain size, but did not meet the H-P linear relationship. This may be attributed to the increase in grain boundaries in the alloy and the dislocation behaviour had little influence on the yield stress of the crystal [30].

$$H = H_0 + Kd^{\frac{1}{2}} \tag{11}$$

where H represents the yield limit of the material, which can usually be represented by hardness HV; H_0 is a constant which represents the lattice friction generated when moving a single dislocation; K is the constant that characterize the influence of grain boundaries on the strength and d is the average grain diameter.

The X-ray diffraction patterns of the samples with pH 6 or 7 have no sharp diffraction peaks. There is a smooth broad peak centred at approximately 2θ = 45 °, indicating an amorphous structure which is long-range disordered. The Co-W coatings with less than ~15 at.% (38.4 wt. %) of W are predominantly crystalline, whereas the coatings with greater than ~20 at.% (43.8 wt. %) of W are predominantly amorphous [33, 37]. The W content of the coatings obtained at pH 6 and 7 in this study is about 44 wt. %, so their structures are predominantly amorphous, which consistent with previous researches. In general, the hardness of amorphous coating is less than that of crystalline one. But for Co-W alloy coating, the hardness is determined by many factors, such as composition, structure, and morphology, so it is possible that the hardness of an amorphous coating is greater than that of a crystalline one. As reported in the literature [37], the hardness of the predominant amorphous coatings

was 480-520 HV, while the hardness of the predominant crystalline coatings crystal was only 430-450 HV.

Table 3. XRD results

pH	2θ (º)			FWHM (º)			Grain size (nm)		
	θ_1	θ_2	θ_3	W_1	W_2	W_3	S_1	S_2	S_3
3	44.580	50.797	74.751	0.474	0.412	0.398	17.912	21.108	24.839
4	44.593	50.850	74.763	0.511	0.451	0.417	16.616	19.287	23.709
5	44.460	51.069	74.643	0.485	0.512	0.591	17.499	17.005	16.715
9	44.541	50.820	74.744	0.516	0.409	0.289	16.452	21.265	34.205

Fig. 13 is a SEM image of the coating prepared at various pH values. As shown in Fig. 13, the pH 3 coating shows loose dendrites morphology with poor adhesion, whose surface is uneven and easy to peel off from the substrate, while its hardness has the minimum value. The coating at pH 7 has a dense and smooth surface with good substrate adhesion, while its hardness has the maximum value. The coating at pH 9 exhibits loose piled blocks morphology, whose hardness is in the middle. The morphology and hardness are consistent, indicating that hydrogen evolution at lower pH and the formation of hydroxide at higher pH might be the reason for the decline of the coating quality, thus affecting the hardness. Consequently, pH 7 is an optimal condition.

All the factors during electrodeposition process affect the structure, content and morphology of the coating, all of these integrated performances in turn results in different hardness. The major reason for this may be that the operating conditions affected the binding mode and complexing form of tungsten, cobalt and citrate, the ease of their discharge, and the rate of nucleation and growth of the reductive metal-containing species. The explanation of the mechanism needs further in-depth specialized study.

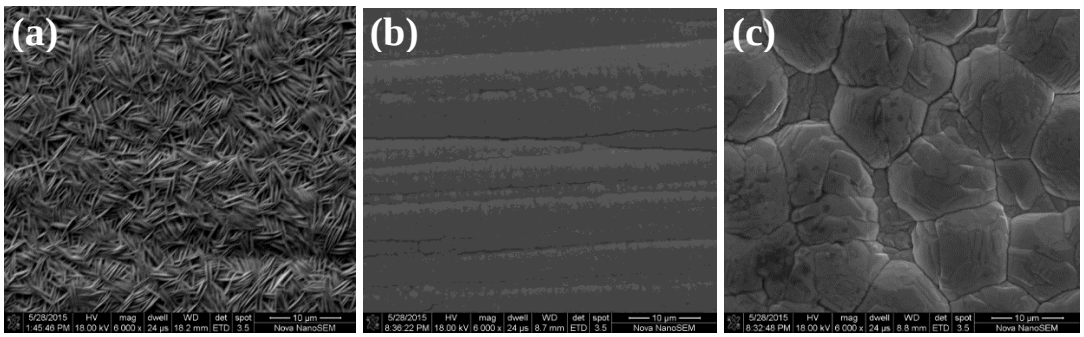

Figure 13. SEM images of coatings obtained at (a) pH = 3; (b) pH = 7; (c) pH = 9 ((g/L)Na_2WO_4 99, $CoSO_4 \cdot 7H_2O$ 56, $C_6H_8O_7 \cdot H_2O$ 80, H_3BO_3 40, Sodium dodecyl sulfate 1; 60 ℃; 500 mA/dm^2).

3.6 Hardness of regenerated coating and primary coating

Co-W alloy coatings (primary coating) were prepared by the same citrate complexing electrodeposition using analytical grade Na_2WO_4 under the same conditions to the coating obtained by

regenerated Na_2WO_4 (regenerated coating) at pH (3-9), temperature (40-80℃) and current density (170-1000 mA/dm^2). The hardness values of these two types of coatings are compared in Fig. 14. Under various conditions, the alloy hardness of primary coating and the regenerated coating are similar, indicating that the citric electrodeposition method can be applied to the recovery of tungsten and cobalt to obtain qualified Co-W alloy coatings with good performance. This research on electrodeposition and characterization of Co-W alloy from regenerated tungsten salt is rarely reported.

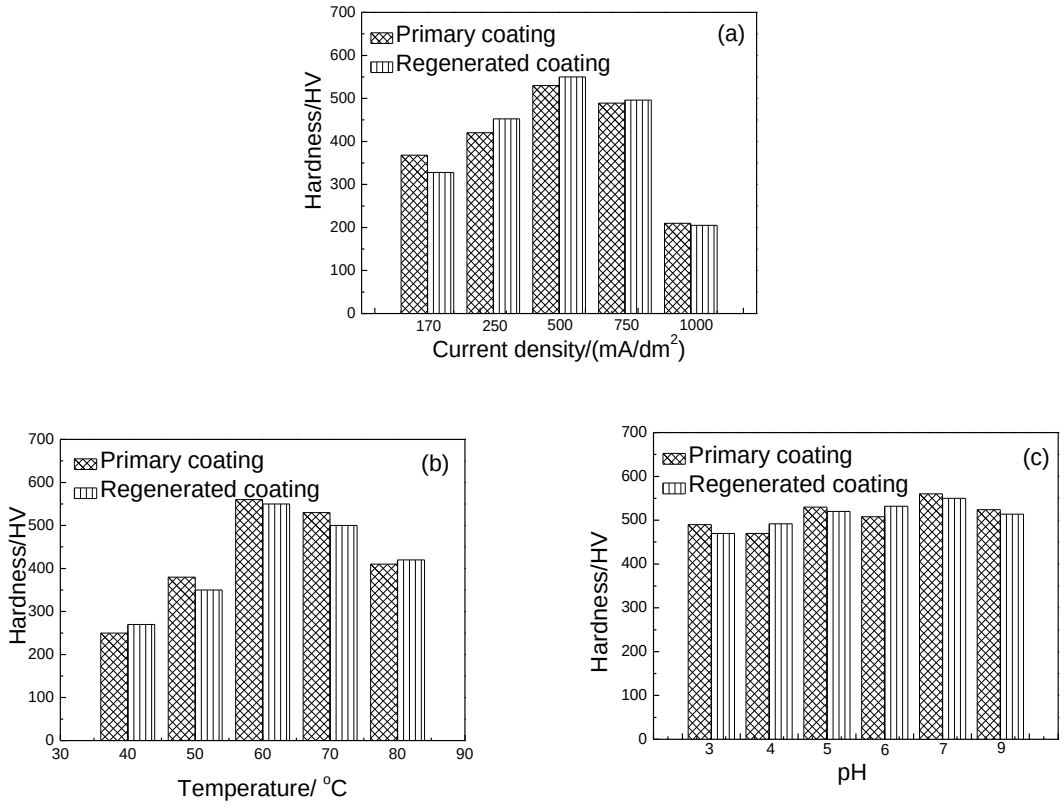

Figure 14. The hardness of Co-W alloy coatings prepared by Na_2WO_4 from analytical grade agent (primary coating) and from regenerated Na_2WO_4 (regenerated coating) under various conditions: (a) current density (170-1000 mA/dm^2); (b) temperature (40-80℃); (c) pH (3-9); the other experimental conditions: pH 7, 60 ℃ and 500 mA/dm^2 when a factor changed

4. CONCLUSIONS

Co-W alloy coating was prepared and studied by electrochemical testing, deposition conditions experiments and performance analysis. The conclusions were as follows:

(1) Cyclic voltammetry showed that tungsten codeposited as Co-W alloy coating by cobalt in the citric acid complexing electrolyte. Suitable amout of tungsten concentration in solution, high temperature and high pH favors the electrodeposition of the electrodeposition of Co-W alloy.

(2) Deposition conditions experiments showed that amorphous Co-W alloy coatings with high W content of 44.2 wt.%, hardness of 550 HV and a complete dense morphology can be obtained by regenerated tungsten salt at 60 ℃, pH 7, and a current density of 500 mA/dm^2. The deposition rate and the current efficiency are 3.487 g/(m^2·h) and 65 %, respectively. The factors during electrodeposition

process affect the structure, content and morphology of the coating, all of these performances in turn lead to different hardness.

(3) The Co-W coating from the regenerated material showed similar hardness compared to the coatings prepared using analytical grade agent, indicating that the regenerated tungsten can be used to prepare qualified Co-W alloy coating.

ACKNOWLEDGEMENTS
This work was supported by National Natural Science Foundation of China (51304010, 51422401).

References

1. European Parliament and Council of the European Union, *Off. J. European Communities*, L37 (2003) 19.
2. E.W. Brooman, *Met. Finish*., 98 (2000) 42.
3. G. Yar-Mukhamedova, M. Vedb, N. Sakhnenko, A. Karakurkchi and I. Yermolenko, *Appl. Surf. Sci*., 383 (2016) 346.
4. S.M. Mayanna, L. Ramesh, B.N. Maruthi and D. Landolt, *J.Mater. Sci. Lett*., 16 (1997) 1305.
5. I. Mizushima, P.T. Tang, H.N. Hansen and M.A.J. Somers, *Electrochim. Acta*, 51 (2006) 6128.
6. O. Younes-Metzler, L. Zhu and E. Gileadi, *Electrochim. Acta*, 48 (2003) 2551.
7. M. Svensson, U. Wahlstrom and G. Holmbom, *Surf. Coat. Technol*., 105 (1998) 218.
8. Z. Galikova, M. Chovancova and V. Danielik, *Chem. Pap*., 60 (2006) 353.
9. M.A.M. Ibrahim, S.S. Abd El Rehim and S.O.Moussa, *J. Appl. Electrochem*., 33 (2003) 627.
10. A. Brenner. Electrodeposition of Alloys, Academic Press, Inc., (1963) New York, USA
11. H. Cesiulis, M. Donten, M.L. Donten and Z. Stojek, *Mater. Sci. Medziagotyra*, 7 (2001) 237.
12. D.P. Weston, S.J. Harris, P.H. Shipway, N.J. Weston and G.N. Yap, *Electrochim. Acta*, 55 (2010) 5695.
13. D.P. Weston, S.J. Harris, H. Capel, N. Ahmed, P.H. Shipway and J.M. Yellup, *Trans. Inst. Met. Finish.*, 88 (2010) 47.
14. M. Donten, H. Cesiulis and Z. Stojek, *Electrochim. Acta*, 45 (2000) 3389.
15. C. Fan, D.L. Piron, A. Steb and P. Paradis, *J. Electrochem. Soc*. 141 (1994) 382.
16. T.M. Sridhar, N. Eliaz and E. Gileadi, *Electrochem. Solid-State Lett*., 8 (2005) C58.
17. M. Donten, *J. Solid State Electrochem*., 3 (1999) 87.
18. M. Donten and Z. Stojek, *J. Appl. Electrochem*., 26 (1996) 665.
19. A.B. Lende and P.S. Kulkarni, *J. Water Process Eng*., 8 (2015) 75.
20. J. W. Kim, W. G. Lee, I. S. Hwang, J. Y. Lee and C. Han, *J. Ind. .Eng. Chem*., 28 (2015) 73.
21. J. Shibata, N. Murayama and M. Niinae, *Geosystem Eng.*, 17 (2014) 120.
22. X. Xi, Z. Nie, K. Xu, L. Ma, G. Chen, X. Zhang and T. Zuo, *Int. J. Refract. Met. H.*, 41 (2013) 90.
23. M. Pourboix, Atlas of electrochemical equilibria in aqueous solutions, Pergamon Press, (1966) NewYork, USA.
24. N.N. Greenwood and A. Earnshow, Chemistry of the Elements, Pergamon Press, NewYork, 1984.
25. J.J. Cruywagan, L. Kruger and E.A. Rohwer, *J. Chem. Soc. Dalton Trans*., 7 (1991) 1727.
26. O. Younes and E. Gileadi, *Electrochem. Solid St. Lett*., 12 (2000) 543.
27. O. Younes, L. Zhu, Y. Rosenberg, Y. Shacham-Diamand and E. Gileadi, *Langmuir*, 17 (2001) 8270.
28. O. Younes and E. Gileadi, *J. Electrochem. Soc*., 149 (2002) C100.
29. O. Younes-Metzler, L. Zhu and E. Gileadi, *Electrochim. Acta*, 48 (2003) 2551.
30. K. Arunsunai Kumar, G. Paruthimal Kalaignan and V.S. Muralidharan, *Appl. Surf. Sci*., 259 (2012)

231.
31. A. Subramania, A.R. Sathiya Priyaa and V.S. Muralidharan, *Int. J Hydrogen Erg*., 32 (2007) 2843.
32. M. Ma, V.S. Donepudi, G. Sandi, Y.K. Sun and J. Prakash, *Electrochim. Acta*, 49 (2004) 4411.
33. N. Tsyntsaru, H. Cesiulis, A. Budreika, X. Ye, R. Juskenas and J.P. Celis, *Surf. Coat. Technol*., 206 (2012) 4262.
34. S.S. Belevskii, H. Cesiulis, N.I. Tsyntsaru and A.I. Dikusar, *Surf. Eng. Appl. Electrochem.*, 46 (2010) 570.
35. H. Cesiulis, A. Budreika, Physicochem, *Mech. Mater.*, 8 (2010) 808.
36. F. Su, C. Liu and P. Huang, *J. Alloy. Compd*., 557 (2013) 228.
37. M. Mulukutla, V.K. Kommineni and S.P. Harimkar, *Appl. Surf. Sci*., 258 (2012) 2886.
38. Z. Ghaferi, K. Raeissi, M.A. Golozar and H. Edris, *Surf. Coat. Technol*., 206 (2011) 497.

39.